Acta Geologica Sinica (English Edition), 2021, 95(4): 1112–1127

Cenozoic Crustally-derived Carbonate-rich Magmatic Rocks in West Junggar, North Xinjiang, Western China: Geochronology, Geochemistry and Tectonic Implications

CHEN Shi[1, 2, *], LIANG Xinxin[1, 2], ZHANG Yuanyuan[3], GUO Zhaojie[3] and QI Jiafu[1, 2]

[1] *State Key Laboratory of Petroleum Resources and Prospecting, China University of Petroleum, Beijing 102249, China*
[2] *College of Geosciences, China University of Petroleum, Beijing 102249, China*
[3] *Key Laboratory of Orogenic Belts and Crustal Evolution, Ministry of Education, School of Earth and Space Sciences, Peking University, Beijing 100871, China*

Abstract: The carbonate-rich magmatic rocks of West Junggar are distributed in the Baijiantan and Darbut ophiolitic mélanges in the forms of extrusive rocks overlying the mélanges and dykes, either along the margins of the mélange or cross-cutting components of mélanges. Chilled margin and flow structures are present. A SHRIMP zircon U-Pb age of 39.7 ± 1.3 Ma indicates that these carbonate-rich rocks in West Junggar were formed during the Eocene. They have low concentrations in REEs, Th, U, Nb, Ta and are characterized by extremely low $\varepsilon_{Nd}(t)$, high $(^{87}Sr/^{86}Sr)_i$ ratios, relatively high $\delta^{18}O_{V\text{-}SMOW}$ values and high $\delta^{13}C_{V\text{-}PDB}$ values, which is similar with most sedimentary carbonates. Furthermore, no contemporaneous mantle-derived silicate rocks have yet been found in West Junggar. The carbonate-rich rocks in West Junggar are thus distinct from mantle-derived carbonatites and are interpreted to result from melting of the Carboniferous sedimentary carbonates at crustal levels, these rocks therefore being referred to as 'crustal carbonatites'. The Eocene crustal carbonatites in West Junggar and other Cenozoic magmatic rocks in North Xinjiang are generally situated along regional strike-slip faults or fault intersections. Therefore, we propose that the reactivation of the Darbut and Baijiantan crustal-scale strike-slip fault zones (ophiolitic mélanges), due to the far-field effects of the Indian-Eurasian collision, enables decompression melting of the underlying continental lithospheric mantle. These resulting melts ascended to the lower crust through the strike-slip faults, causing partial melting of the Carboniferous carbonaceous sediments. The crustal carbonatites in West Junggar provide a new piece of evidence for Cenozoic magmatism in North Xinjiang and are also significant for the investigation of tectono-magmatic relations in North Xinjiang and the Central Asian Orogenic Belt.

Key words: crustal carbonatite, strike-slip fault, decompressional melting, Cenozoic, West Junggar

Citation: Chen et al., 2021. Cenozoic Crustally-derived Carbonate-rich Magmatic Rocks in West Junggar, North Xinjiang, Western China: Geochronology, Geochemistry and Tectonic Implications. Acta Geologica Sinica (English Edition), 95(4): 1112–1127. DOI: 10.1111/1755-6724.14772

1 Introduction

Carbonatites are igneous rocks with a rare distribution on Earth. It has been widely accepted since the mid-1960s that carbonatite magmas are ultimately derived from the mantle, particularly when they have close spatial and temporal relationships and geochemical links to other mantle-derived silicate rocks, such as dunite, kimberlite, lamprophyre and pyroxenite (e.g., Deines, 1989; Bizimis, 2001; Bell and Rukhlov, 2004; Santosh and Omori, 2008; Sharygin et al., 2015). The mantle-derived carbonatites are considered to represent primary melts derived by partial melting of carbonated peridotite and carbonated eclogite (Dalton and Wood, 1993; Hammouda, 2003; Downes et al., 2005) and/or are the result of fractional crystallization and liquid immiscibility of mantle-derived silicate parental melts (Veksler et al., 1998; Solovova et al., 2005; Rosatelli et al., 2007). However, in some other cases, carbonatites show different chemical and isotopic compositions from these mantle-derived carbonatites. Such carbonatites have been interpreted to be generated by the melting of sedimentary carbonates (Zhao et al., 2004; Liu et al., 2006; Ren at al., 2007; Wan et al., 2008; Dong et al., 2009; Chen et al., 2010).

It is well-known that carbonatite occurrences are confined to intracontinental rift-related environments, such as the East African Rift (e.g. Bell and Tilton, 2001; Pirajno, 2015) and some (post-) collisional settings (e.g. Chakhmouradian et al., 2008; Xu et al., 2011). Although carbonatites have been found on all continents and in two oceanic localities (Bell et al., 1998; Bell and Tilton, 2002; Woolley, 2003), the occurrence of carbonatites in China are rare, with a few exceptions such as the North China Craton (Wan et al., 2008; Xu et al., 2011), the Tarim Block (Zhang et al., 2007), the Qingling Orogen (Xu et al., 2014) and the Mianning–Dechang carbonatite belt in the Himalayan collision zone (Hou et al., 2006, 2015; Liu et al., 2006, 2015, 2017).

The Central Asian Orogenic Belt (CAOB) (Fig. 1a), also called the Altaid Tectonic Collage or Central Asian

* Corresponding author. E-mail: chenshi4714@163.com

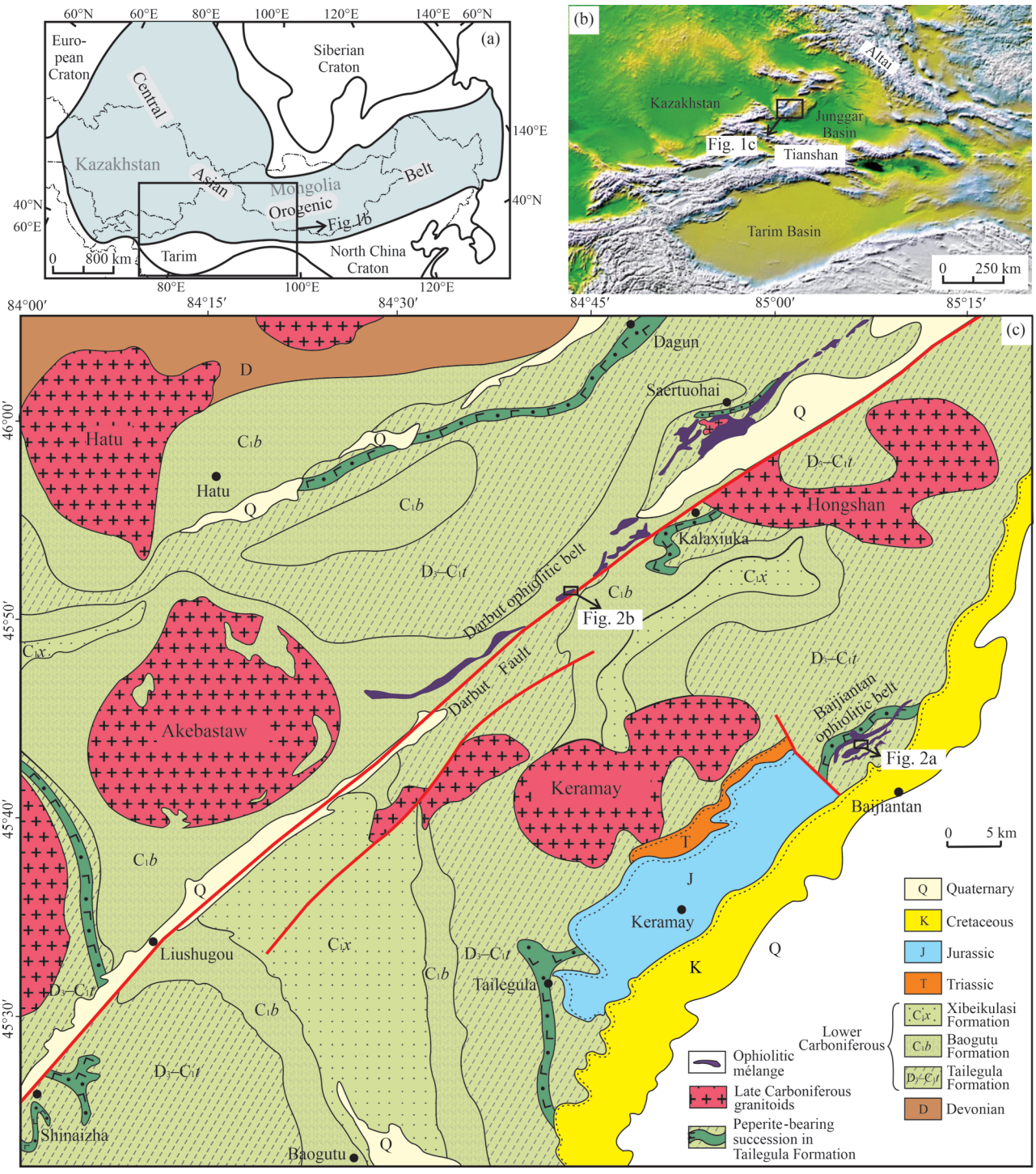

Fig. 1. Regional map of CAOB and West Junggar.
(a) Simplified sketch map of Central Asian Orogenic Belt (modified after Sengör et al., 1993); (b) digital elevation model of North Xinjiang area; (c) geological map of West Junggar (modified after the geological map of 1:200,000 produced by XBGMR, 1966).

Orogenic System (Sengör et al., 1993; Sengör and Natalin, 1996; Yakubchuk, 2004), is one of the largest accretionary orogens in the world and was formed by Neoproterozoic–Paleozoic successive amalgamations of allochthonous oceanic and pericratonic terranes, island arcs and possibly microcontinents (Coleman 1989; Jahn 2004; Windley et al., 2007; Xiao et al., 2008), separating the Siberian craton from the Tarim and North China cratons. No carbonatite has previously been reported in the North Xinjiang region within the CAOB, which is a key area for study of the tectonic evolution of the CAOB.

In this study, we report a special type of carbonate-rich magmatic rock in West Junggar in North Xinjiang, investigating its petrological, geochronological,

geochemical and isotopic characteristics. Deciphering the genesis of this rock-type (referred to as crustal carbonatite) is considered to be of invaluable significance for understanding the tectono-magmatic relations and crust-mantle interaction in West Junggar.

2 Geological Setting

2.1 General aspects

The West Junggar region, surrounded by the Altai Orogen to the north, the Tianshan Orogen to the south, the Kazakhstan Plate to the west and the Junggar Basin to the east, is regarded as a window on the evolutionary history of the CAOB (Fig. 1) (Windley et al., 2007; Xiao et al., 2010; Yi et al., 2015). The principal rock assemblages in West Junggar include Paleozoic ophiolitic mélanges and Carboniferous sedimentary formations, both of which are intruded by sub-circular Late Carboniferous granitoid plutons (Fig. 1c) with a strongly positive ε_{Nd} (Chen and Arakawa, 2005). Regionally, Late Devonian (ca. 364 Ma) peperitic basalt lavas are interbedded with sedimentary rocks, passing up into a 5 km thick Carboniferous succession of shallowing-upwards clastic facies that include some volcanic rocks. These continuous stratigraphic sections have been divided (from bottom upwards) into the Tailegula, Baogutu and Xibeikulasi formations (Chen et al., 2013) and are distributed regionally over a distance of 100 km on both sides of the Darbut Fault (Fig. 1c). The northeast-striking Darbut Fault is known as a Permian or even younger high-angle transcurrent strike-slip fault across the whole West Junggar region (Allen et al., 1995), extending for more than 200 km (Fig. 1c).

The other striking geological feature in West Junggar is the occurrence of two parallel NE-trending subvertical belts of ophiolitic rocks: the Baijiantan and Darbut ophiolitic mélanges (Fig.1c) (Zhang et al., 2011; Choulet et al., 2012; Chen et al., 2014). These ophiolitic mélanges act as two parallel, steeply-dipping fault zones, bounding a foliated serpentinite matrix made up of a range of deformed sedimentary and igneous blocks, which are in tectonic contact with regionally-distributed Late Devonian –Early Carboniferous (D_3–C_1) ocean floor peperitic basalts and overlying deep-water Carboniferous sedimentary successions (Chen et al., 2013). The Baijiantan ophiolitic mélange zone ranges from 0.5 to ~2 km in width. The structure of the Baijiantan mélange is dominated by two steeply-dipping master fault-zones which extend about 7 km at a NE bearing of 50° with a few branch faults (Fig. 1c). The Darbut ophiolitic mélange outcrops for approximately 105 km in length and < 5 km in width, extending along the north side of the NE-trending Darbut Fault, striking NE (Fig. 1c). About 10 tectonic slices of mélange are distributed along a 100 km portion of the fault from the Akebastaw granite pluton in the west to the Kalaxiuka and Saertuohai areas in the east (Fig. 1c). A Sm -Nd isochron age of 395 ± 12 Ma (Zhang and Huang, 1992) and a laser ablation inductively coupled plasma mass spectrometry (LA-ICP-MS) zircon U-Pb age of 391 ± 6 Ma (Gu et al., 2009) were obtained from gabbroic rocks within the Darbut ophiolite. Two sets of sensitive high-resolution ion microprobe (SHRIMP) zircon U-Pb dates of 332 ± 14 Ma and 414 ± 9 Ma were reported from a gabbro from the Baijiantan ophiolite (Xu et al., 2006). Recently, multiple clusters in SHRIMP zircon ages from single gabbro blocks in the two mélanges at 376 ± 5 Ma, 363 ± 5 Ma, 354 ± 5 Ma, and 338 ± 3 Ma were also reported (Chen et al., 2014).

2.2 Field occurrence of the carbonate-rich magmatic rocks

The carbonate-rich magmatic rocks in West Junggar are distributed across the Baijiantan and Darbut ophiolitic mélanges, in the form of extrusive rocks and dykes, respectively (Fig. 2).

In the Baijiantan ophiolitic mélange, the outcrops of effusive carbonate-rich magmatic rocks appear as a series of circular to subcircular cones ranging from 2500 m^2 to 40000 m^2 (Fig. 2a). Most of these extrusive bodies occur within the Baijiantan mélange, but some also occur within the Carboniferous strata, close to the fault zone that separates the two geological units. Compared to the mélanges that are susceptible to weathering, the carbonate-rich magmatic rocks commonly appear as a pale red color on hilltops with underlying mélanges and/or Carboniferous strata (Fig. 3a). The extrusive carbonate-rich rocks in the Baijiantan area are massive with local flow structures (Fig. 3b). Chilled margins are also present in contact with the Carboniferous sandstone, where coarse -grained calcite has locally been observed (Fig. 3c).

In the Kalaxiuka area around the Darbut ophiolitic mélange, the carbonate-rich magmatic rocks occur as dykes (Fig. 2b). Some of the dykes were emplaced along the structural boundary between the Darbut ophiolitic mélange and the surrounding Carboniferous successions (Fig. 3d, e). These dykes vary from 20 m to 50 m in width and dip steeply with ~80° dip, extending about 800–1500 m in E–W and SE–NW directions. Some dykes split and were emplaced in Carboniferous strata (Fig. 2b). There are also some small (< 300 m in length) vertical dykes within the Darbut ophiolitic mélange, which cross-cut all the components in the mélanges (Figs. 2b, 3f). The carbonate-rich dykes appear massive without flow structures.

3 Analytical Methods

3.1 SHRIMP zircon analyses

Separation of zircon grains was conducted using conventional heavy liquid and magnetic techniques. The individual crystals, together with the TEMORA standard zircons, were mounted in epoxy resin and then polished to approximately half their thickness. All zircon grains were photographed under both reflected and transmitted light using an optical microscope. Cathodoluminescence (CL) images of zircon grains were obtained using a scanning electron microscope (SEM) at Peking University in order to reveal the internal textures to best identify the optimum for analysis.

U-Th-Pb analyses of zircon were measured using the SHRIMP II in the Beijing SHRIMP Centre, Institute of Geology, Chinese Academy of Geological Sciences, Beijing, China. Instrumental conditions and measurement

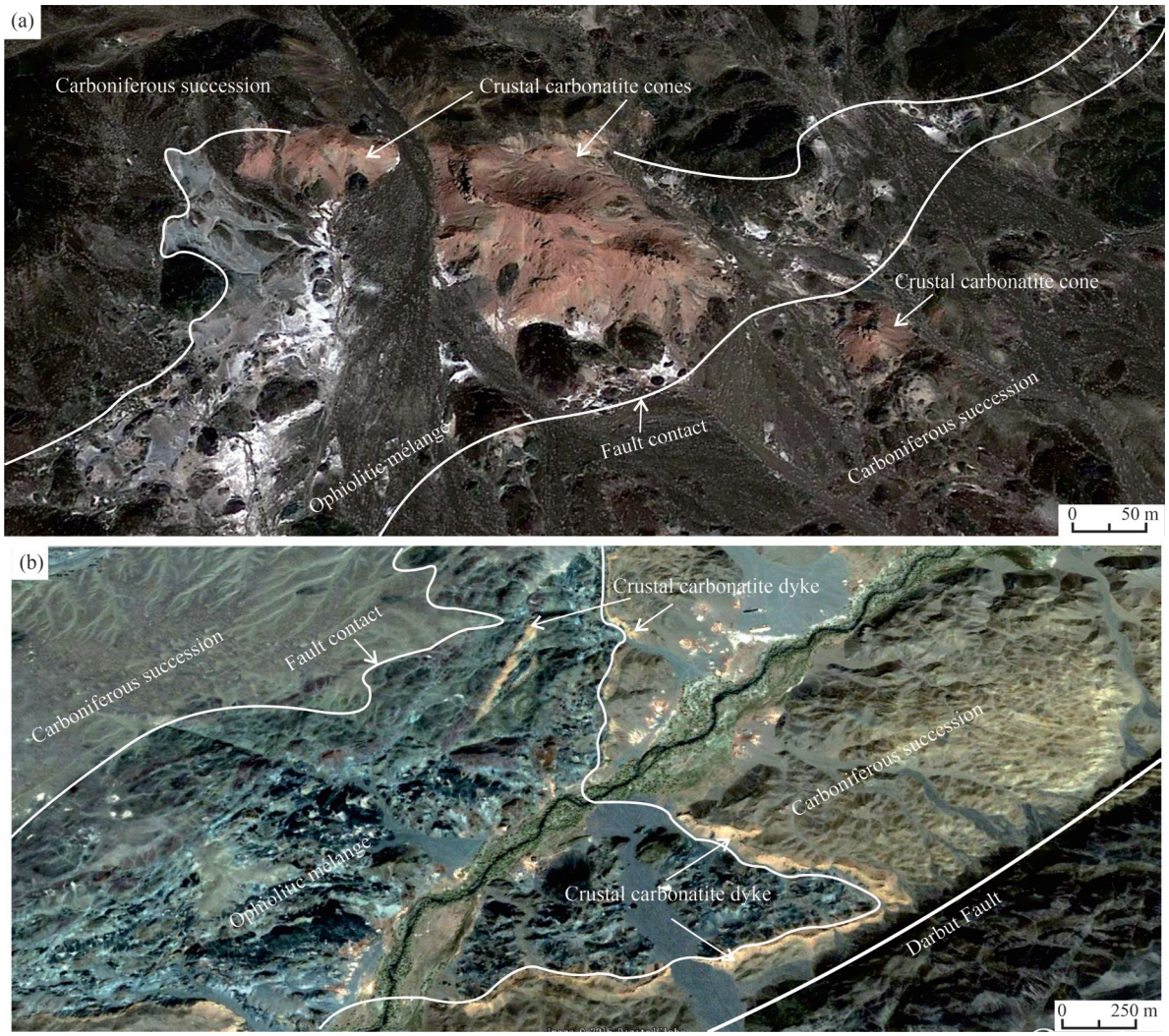

Fig. 2. Remote sensing images of the Baijiantan area (a) and Kalaxiuka in the Darbut area (b), showing the occurrences of carbonatites from West Junggar.

(a) The effusive carbonatite outcrops are shown as a series of circular to subcircular cones. Some carbonatite bodies occur within the Baijiantan ophiolitic belt and overlie the Baijiantan mélange along the fault. Some bodies overlie the Carboniferous successions; (b) carbonatite occurs as subvertical dykes in the Kalaxiuka area. Some of them are emplaced along the structural boundary between the Darbut ophiolitic mélange and the surrounding Carboniferous succession and some within the mélanges.

procedures were the same as those described by Compston et al. (1992). Spot size was approximately 20 μm in diameter and the data for each spot were collected in sets of five scans. Common Pb corrections were made using measured ^{204}Pb. The decay constants and present-day ^{238}U/^{235}U values given by Steiger and Jäger (1977) were used. The uncertainties given for individual analyses (ratios and ages) were at the 1σ level, whereas the uncertainties in calculated weighted mean ages were reported with 95% confidence.

3.2 Petrology and whole-rock analysis

All samples were investigated in detail using an optical microscope. The selected samples were then analysed using a FEI Quanta-650FEG variable-pressure scanning electron microscope (SEM), equipped with energy-dispersive spectroscopy (EDS) and a JXA-8100 electron microprobe (EMP) in Peking University, China. The operating conditions of the EMP were at 15 kV with a beam current of 10 nA and diameter of 1 μm.

Major elements were determined on fused glass disks by a Phillips PW 1500 X-ray fluorescence spectrophotometer in the Key Laboratory of Orogenic Belts and Crustal Evolution, Peking University. The precision and accuracy of the major element data as determined on the Chinese whole-rock basalt standard GSR-3 (Xie et al., 1985) are ≤ 3% and ca. 5% (2σ), respectively. Trace and rare earth elements (REE) of the samples were determined using ICP-MS on an ELEMENT -2 mass spectrometer at the Geological Analysis and Research Centre of the Nuclear Industry of China. The analysis inaccuracy was estimated to be < 2%, the detection limit for these elements being 0.05 ppm. Sr-Nd-Pb and C-O isotopic analyses were also performed at the

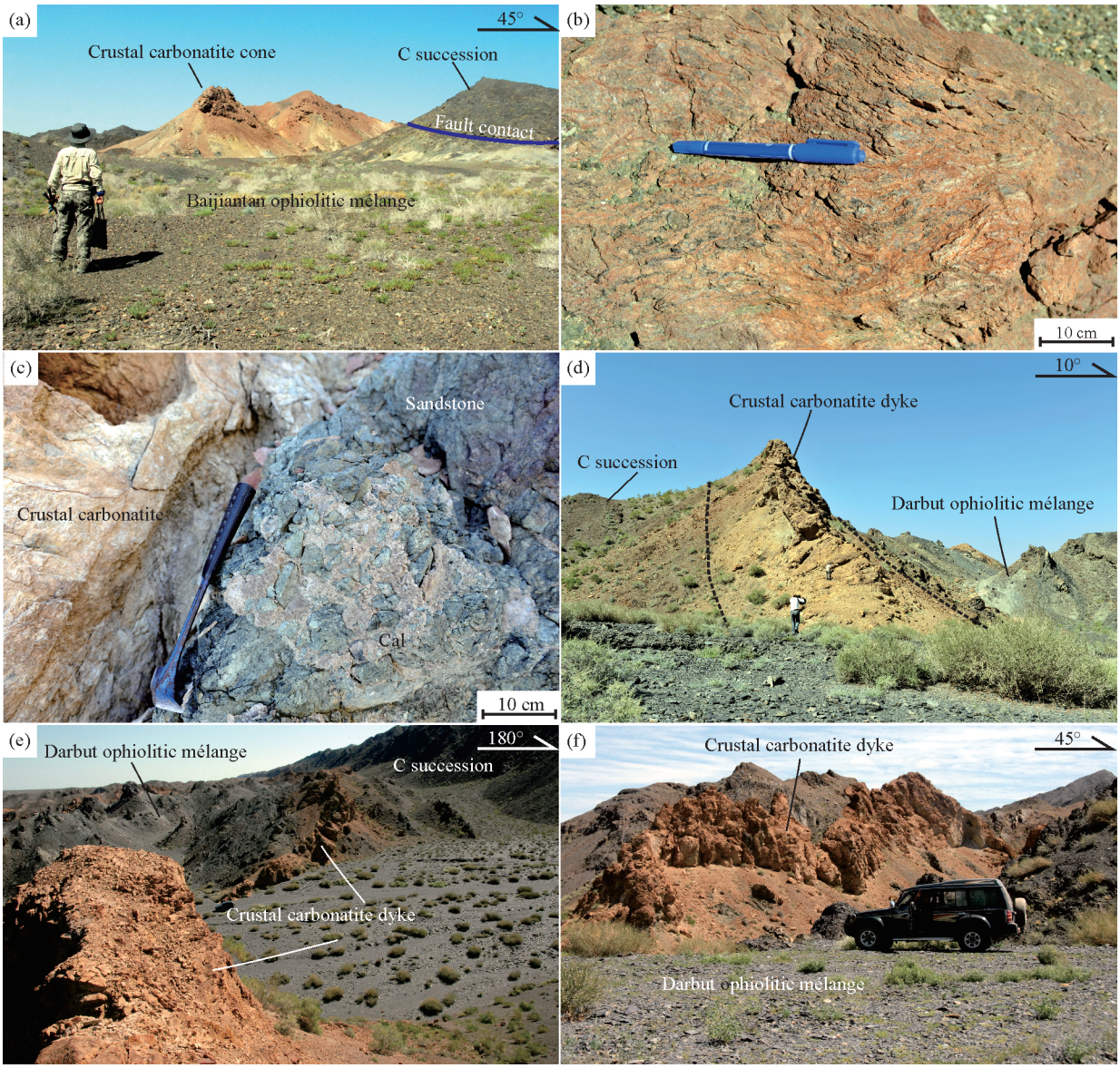

Fig. 3. Field outcrops of the carbonatites from West Junggar.
(a) The Baijiantan ophiolitic mélange and Carboniferous succession were overlain unconformably by the carbonatite cone; (b) flow structures in the carbonatite from the Baijiantan area; (c) light-colored baked rim formed in the Carboniferous sandstone at the contact with the carbonatites. Coarse-grained calcite was developed in the sandstones; (d) sub-vertical carbonatite dyke emplaced along structural boundaries between the Darbut ophiolitic mélange and the surrounding Carboniferous succession in the Kalaxiuka area; (e) the carbonatite dykes extend along the boundary of the Darbut ophiolitic mélange about 800–1500 m in an E–W direction; (f) vertical carbonatite dyke emplaced within the Darbut ophiolitic mélange and cross-cutting the matrix and blocks of the mélange.

Geological Analysis and Research Centre of the Nuclear Industry of China. Detailed description of the preparation procedures and the techniques for the analytical methods are provided in supplementary material.

4 Results

4.1 Petrology

More than 50 modal% carbonate minerals of magmatic origin were present in most samples, which were identified as carbonatites, according to the definition of the IUGS (Le Maitre, 2002) and Mitchell (2005, lower limit of carbonate is 30%).

4.1.1 Extrusive carbonatite

There are two types of extrusive carbonatite occurring in the Baijiantan ophiolitic mélange, based on their mineral compositions. The first type is composed of dolomite (~35%), calcite (~15%), with accessory siderite (~5%) and non-carbonate minerals (Figs. 4a, b). Most non-carbonate minerals are quartz (~35%), enstatite (~10%) with small amounts of chromite, magnetite and apatite. The other type of carbonatite (Figs. 4c–e) mainly consists of dolomite and calcite, with some accessory minerals, including quartz, enstatite, chromite, spinel and magnetite. Samples from both types appear massive with local flow structures (Fig. 4f).

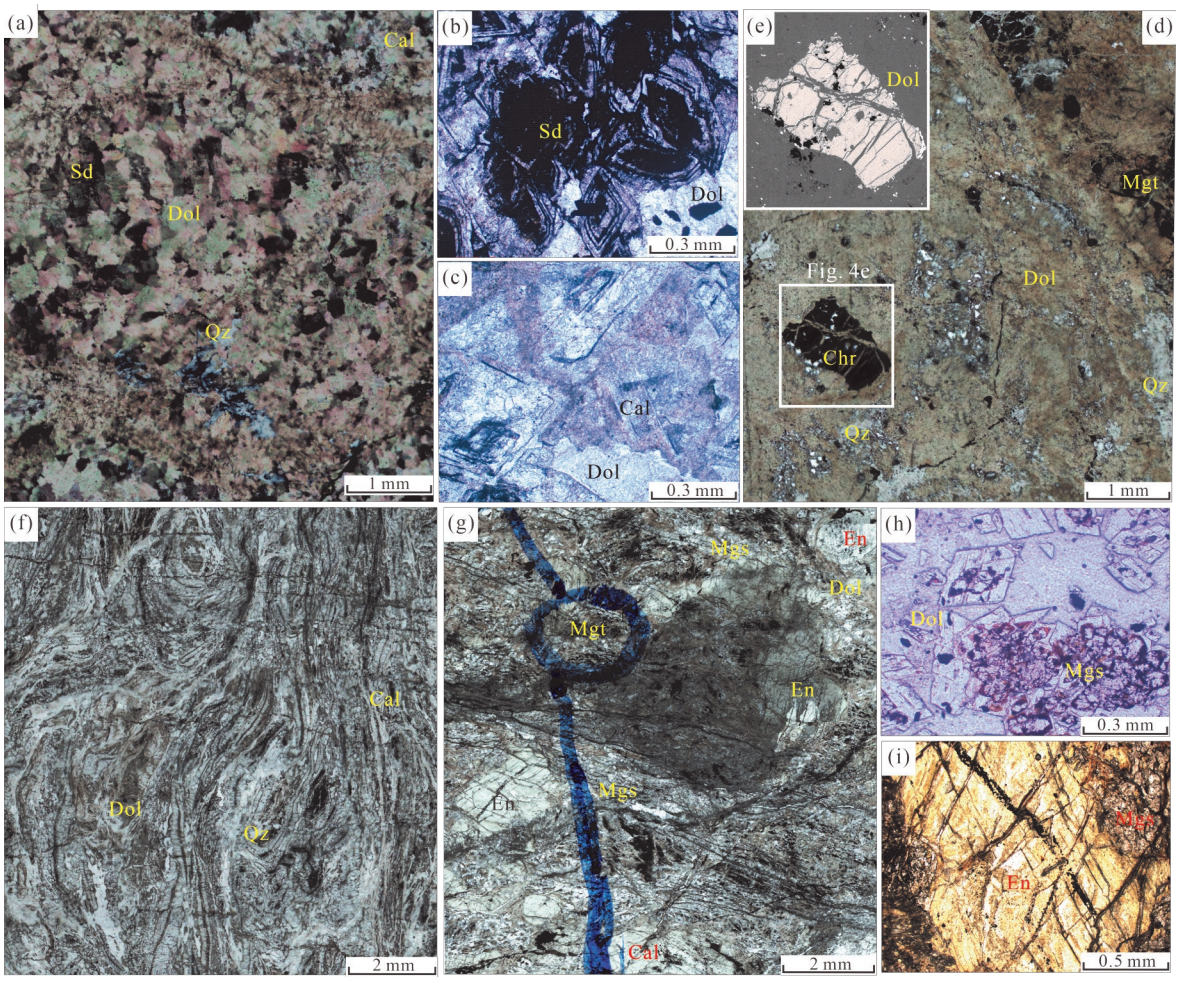

Fig. 4. Microphotographs of extrusive (a–f) and intrusive (g–i) carbonatites.
(a) Under cross-polarized light; (b–i) under plane-polarized light; (e) BSE image of the enlarged area in (d). Abbreviations: Cal = calcite; Chr = chromite; Dol = dolomite; En = enstatite; Mgs = magnesite; Mgt = magnetite; Qz = quartz; Sd = siderite.

4.1.2 Carbonatite dykes

Compared to extrusive carbonatite, the carbonate minerals (~45%–55%) in the dykes within the Darbut ophiolitic mélanges are magnesite (~35%), calcite (~15%) and a small amount of dolomite (~5%) (Fig. 4g–i). The non-carbonate minerals include quartz (~20%), enstatite (~20%) and accessory chromite, spinel and magnetite.

4.2 U-Pb Dating

One extrusive sample (XZ-18) from the Baijiantan area was chosen for zircon SHRIMP U-Pb dating (Table 1). The zircons are mostly subhedral and short prismatic crystals with an average length of 50–100 μm. All zircons are transparent and show oscillatory zoning, indicative of magmatic growth (Fig. 5a). Most grains appear to have a core, with a break in growth pattern or zoning. Some cores have igneous zoning and some appear dark in color. In order to determine the formation age of the carbonatite, a total of eight spots were selected on the zircon grains, by avoiding the core area of the zircon. Two sets of age data for the cores of zircon were also obtained, to help investigate the source of these carbonatites.

All 8 analyses have moderate U contents with variable Th/U (0.36–1.06). These 8 concordant analyses yielded an Eocene weighted mean $^{206}Pb/^{238}U$ age of 39.7 ± 1.3 Ma (MSWD = 0.54) (Fig. 5b). Dating of the cores of the zircon grains yielded Carboniferous $^{206}Pb/^{238}U$ ages of 339 ± 12 Ma and 309 ± 10 Ma.

4.3 Major and trace elements

All the carbonatite samples in West Junggar have variable SiO_2 content (24.52–53.52 wt% for extrusive samples, and 30.66–35.85 wt% for intrusive samples) (Table 2). Four extrusive carbonatite samples show relatively high CaO (12.49–28.59 wt%) and low MgO (5.78–21.08 wt%), compared with the intrusive samples. Samples from carbonatite dykes show similar major element compositions with relatively high MgO (24.83–27.03 wt%) but relatively low CaO (0.03–3.57 wt%). There are small amounts of Al_2O_3 (~0.7–1.5 wt%) and TFe_2O_3 (~3.4–7.5 wt%, slightly higher in the intrusive rather than the extrusive samples) and very low concentrations of K, Na, Mn, Ti and P in all carbonatite samples.

The concentrations of most incompatible elements, e.g. REEs, in the carbonatite in West Junggar are remarkably

low, compared with the mantle-derived carbonatite (Bizimis, 2001). All the carbonatite samples in West Junggar show flat REE patterns with a positive Eu anomaly in most of the samples (Fig. 6a). Most of the incompatible elements in the carbonatites are at levels less than that of the primitive mantle, with distinct positive Ba, U and Sr anomalies (Fig. 6b) in the primitive mantle-normalized spider diagram. Nb is slightly depleted for most of the samples and no Zr and Hf anomalies were observed.

4.4 Isotopic results

The Sr-Nd-Pb isotopic compositions of the carbonatite in West Junggar are listed in Table 3 and shown in Figure

Table 1 SHRIMP U-Pb data of crustal carbonatite sample XZ-18 from the Baijiantan area in West Junggar

Spot	U (ppm)	Th (ppm)	$^{206}Pb^a$ (ppm)	$^{206}Pb_c{}^b$ (%)	$^{232}Th/^{238}U$	$^{207}Pb^a/^{206}Pb^a$	Error^c (%)	$^{207}Pb^a/^{235}U$	Error (%)	$^{206}Pb^a/^{238}U$	Error (%)	Error corr	$^{206}Pb/^{238}U$ age (Ma)	
XZ-18-1	1367	1143	7.31	4.41	0.86	0.0458	15	0.0376	15	0.00595	2.5	0.162	38.2	1
XZ-18-2	933	986	12.8	57.19	1.09	0.021	320	0.019	320	0.00684	3.8	0.012	43.5	4
XZ-18-3	996	574	5.78	4.88	0.60	0.0516	5.4	0.0458	6	0.00643	2.6	0.437	41	1.1
XZ-18-4	965	548	7.33	29.07	0.59	0.042	27	0.037	28	0.00627	3.2	0.115	40	1.4
XZ-18-5	577	586	3.58	13.72	1.05	0.0438	12	0.0376	12	0.00623	2.7	0.223	40	1.1
XZ-18-6	1289	837	7.5	10.85	0.67	0.0465	14	0.0387	14	0.00604	2.9	0.204	38.7	1.2
XZ-18-7	815	783	6.41	31.61	0.99	0.0407	23	0.0351	23	0.00627	2.5	0.110	40	1.1
XZ-18-8	1195	426	18.1	63.18	0.37	0.02	130	0.018	130	0.00651	2.5	0.019	40.9	1.8
XZ-18-9	68	34	3.22	10.95	0.52	0.057	25	0.39	25	0.0494	2.8	0.112	309	9
XZ-18-10	67	35	3.72	15.91	0.54	0.061	25	0.46	26	0.0547	3	0.116	339	12

Notes: a, radiogenic Pb content; b, common Pb content; c, errors are 1-sigma.

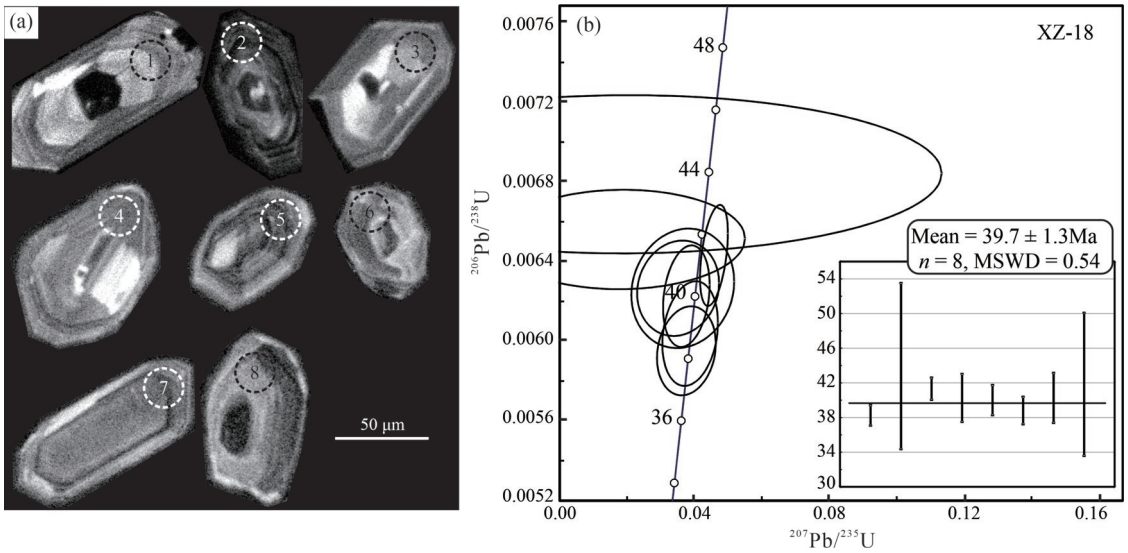

Fig. 5. (a) Cathodoluminescence (CL) images and (b) concordia diagram for zircons from West Junggar extrusive carbonatite sample XZ-18.

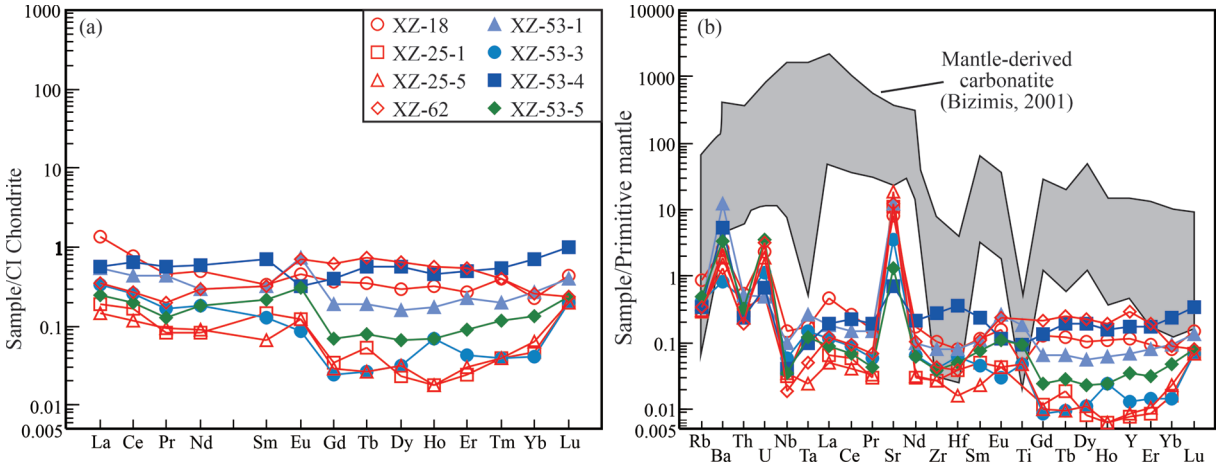

Fig. 6. (a) Chondrite-normalized REE diagram and (b) primitive mantle-normalized incompatible element diagram for the carbonatite rocks from West Junggar (normalizing values are from Sun and McDonough, 1989). Data of mantle-derived carbonatite from Bizimis, 2001.

Table 2 Major (wt%) and trace element (ppm) concentrations of the crustal carbonatite from West Junggar

Sample	XZ-18	XZ-25-1	XZ-25-5	XZ-62	XZ-53-1	XZ-53-3	XZ-53-4	XZ-53-5
Occurrence	Extrusive body				Intrusive dyke			
SiO_2	48.04	24.52	30.21	53.52	30.66	30.97	35.85	34.47
Al_2O_3	1.00	0.76	1.50	0.80	1.14	0.94	0.95	0.73
TFe_2O_3	3.74	6.05	4.16	3.36	7.01	6.04	7.54	6.03
CaO	13.93	12.49	28.59	13.46	3.42	3.57	0.03	0.37
MgO	10.19	21.08	5.78	7.85	24.83	25.11	27.03	26.35
K_2O	0.06	0.05	0.07	0.06	0.04	0.04	0.03	0.04
Na_2O	0.03	0.01	0.04	0.03	0.02	0.01	0.01	0.02
MnO	0.198	0.095	0.201	0.071	0.127	0.094	0.096	0.099
TiO_2	0.009	0.003	0.010	0.003	0.026	0.004	0.014	0.016
P_2O_5	0.002	0.005	0.007	0.002	0.005	0.006	0.007	0.007
LOI	22.37	34.37	28.82	20.52	32.19	32.66	27.86	31.34
Total	99.58	99.43	99.38	99.67	99.47	99.44	99.41	99.47
Li	9.66	1.55	2.11	6.63	25	10.5	29.1	22
Be	0.167	0.085	0.027	0.061	0.132	0.167	0.039	0.174
Sc	4.6	2.61	3.37	4.12	7.32	3.22	8.08	5.91
V	31.7	14	18.7	19	25.7	17.3	44.3	34.8
Cr	1336	2249	4531	499	1358	2640	2105	1580
Co	72.4	81.6	60.7	57	76.4	85.6	91.2	73.9
Ni	1186	1405	954	584	1364	976	1553	1351
Cu	9.09	8.19	6.78	20.2	11.7	25.3	15.4	12.1
Zn	28.9	24.6	26.2	33.4	35.1	23.3	34.1	34.2
Ga	1.06	0.479	0.854	0.949	1.37	0.586	1.09	1.17
Rb	0.544	0.182	0.193	0.211	0.242	0.268	0.212	0.316
Sr	166	231	400	255	258	75.1	15.1	28.3
Y	0.526	0.034	0.039	1.33	0.305	0.058	0.777	0.154
Nb	0.103	0.022	0.025	0.013	0.069	0.042	0.029	0.025
Mo	1.29	0.249	0.258	1.46	0.026	0.076	0.067	0.129
Cd	0.059	0.006	0.038	0.029	0.031	0.017	0.008	0.007
In	0.003	0.003	0.002		0.004	0.003	0.004	0.003
Sb	0.386	2.31	2.99	10.6	3.4	7.92	3.18	7.74
Cs	0.026	0.028	0.018	0.02	0.143	0.029	0.132	0.154
Ba	17.8	13.5	16.7	9.28	86.5	5.72	37.5	23.5
La	0.324	0.044	0.035	0.082	0.127	0.08	0.133	0.059
Ce	0.46	0.102	0.073	0.164	0.263	0.158	0.396	0.119
Pr	0.043	0.008	0.009	0.019	0.041	0.016	0.053	0.012
Nd	0.23	0.039	0.042	0.136	0.135	0.086	0.281	0.083
Sm	0.051	0.022	0.01	0.049	0.048	0.02	0.107	0.033
Eu	0.026	0.007	0.007	0.04	0.043	0.005	0.019	0.018
Gd	0.074	0.007	0.006	0.125	0.039	0.005	0.081	0.014
Tb	0.013	0.002	0.001	0.027	0.007	0.001	0.021	0.003
Dy	0.076	0.006	0.008	0.161	0.04	0.008	0.141	0.017
Ho	0.018	0.001	0.001	0.032	0.01	0.004	0.026	0.004
Er	0.045	0.004	0.005	0.09	0.038	0.007	0.083	0.015
Tm	0.01	0.001	0.001	0.01	0.005	0.001	0.014	0.003
Yb	0.039	0.008	0.011	0.044	0.045	0.007	0.119	0.023
Lu	0.011	0.005	0.005	0.006	0.01	0.005	0.025	0.006
Ta	0.007	0.007	0.001	0.002	0.011	0.006	0.004	0.005
W	0.129	0.496	0.459	0.062	0.053	0.18	0.032	0.077
Tl	0.024	0.002	0.005	0.005	0.007	0.001	0.003	0.003
Pb	1.62	0.424	0.526	4.04	0.398	0.489	0.319	0.322
Bi	0.009	0.005	0.003	0.008	0.003	0.002	0.005	0.003
Th	0.045	0.026	0.02	0.016	0.044	0.037	0.02	0.027
U	0.049	0.011	0.04	0.065	0.01	0.023	0.014	0.074
Zr	1.15	0.294	0.302	0.467	0.889	0.448	3.17	0.421
Hf	0.024	0.012	0.005	0.012	0.025	0.019	0.112	0.015

3. Initial $^{87}Sr/^{86}Sr$ and $^{143}Nd/^{144}Nd$ ratios were calculated using 40 Ma for the carbonatite, and Pb isotopic data were corrected to 40 Ma for post-crystallization decay of Th and U. The carbonatites are characterized by relatively high $(^{87}Sr/^{86}Sr)_i$ ratios of 0.7048–0.7061, low $(^{143}Nd/^{144}Nd)_i$ ratios of 0.51174–0.51243 and a negative $\varepsilon_{Nd}(t)$ range of −2.98 to −16.58. The low $\varepsilon_{Nd}(t)$ and high $(^{87}Sr/^{86}Sr)_i$ ratios of the carbonatite in West Junggar distinguish them from most of the reported young (< 200 Ma) carbonatites worldwide (Fig. 7a) that have positive $\varepsilon_{Nd}(t)$ and low $(^{87}Sr/^{86}Sr)_i$ ratios, e.g. those from the East African Rift Zone (Bell and Tilton, 2001) and oceanic carbonatites from the Cape Verde and Canary Islands (Hoernle et al., 2002).

All analyzed samples were characterized by limited ranges of $^{206}Pb/^{204}Pb$, $^{207}Pb/^{204}Pb$ and $^{208}Pb/^{204}Pb$ ratios (18.272–18.532, 15.537–15.595 and 38.125–38.521, respectively), which were distinct from the ranges of the reported carbonatites around the world (Bell and Tilton, 2001; Hoernle et al., 2002) (Fig. 7b). In the $^{206}Pb/^{204}Pb$ vs. $^{208}Pb/^{204}Pb$ diagram, the carbonatites in West Junggar fell within the continental field (Fig. 7c).

Table 3 Sr-Nd-Pb and C-O isotopes of the crustal carbonatite from West Junggar

Sample	XZ-18	XZ-25-1	XZ-25-5	XZ-62	XZ-53-1	XZ-53-3	XZ-53-4	XZ-53-5
Rb		0.05	0.03		0.062	0.104		0.116
Sr		209	397		237	66.6		23.9
Sm		0.005	0.005		0.029	0.01		0.014
Nd		0.032	0.022		0.118	0.053		0.059
$^{87}Rb/^{86}Sr_m$[a]		0.0007	0.0002		0.0008	0.0045		0.014
$^{87}Sr/^{86}Sr_m$[a]		0.7055	0.7054		0.7048	0.7056		0.7061
$^{147}Sm/^{144}Nd_m$[a]		0.1	0.1454		0.1467	0.1122		0.1469
$^{143}Nd/^{144}Nd_m$[a]		0.51176	0.51203		0.51247	0.51192		0.51233
$^{87}Sr/^{86}Sr_i$[b]		0.7055	0.7054		0.7048	0.7056		0.7061
$^{143}Nd/^{144}Nd_i$[b]		0.51174	0.51199		0.51243	0.51189		0.51229
$\varepsilon_{Nd}(t)$[b]		−16.58	−11.60		−2.98	−13.56		−5.70
$^{208}Pb/^{204}Pb$[c]	38.125	38.251	38.223		38.308	38.521	38.251	38.336
$^{207}Pb/^{204}Pb$[c]	15.537	15.588	15.556		15.574	15.595	15.568	15.572
$^{206}Pb/^{204}Pb$[c]	18.292	18.523	18.291		18.312	18.361	18.272	18.452
$\delta^{13}C_{V\text{-}PDB}$ (‰)	−5.9	−6	−7.1	−5.3	−5.6	−6.5	−3.6	−7.7
$\delta^{18}O_{V\text{-}PDB}$ (‰)	−9.4	−10.6	−10.9	−10	−9.8	−8.5	−7.3	−10.1
$\delta^{18}O_{V\text{-}SMOW}$ (‰)	21.2	20	19.7	20.6	20.8	22.1	23.4	20.5

Notes: a, measured value; b, initial value. The initial Sr and Nd isotopic ratios was ca lculated using the age of 40 Ma; c, Pb isotopic compositions have been corrected for postcrytallization decay of Th and U; V-PDB, Vienna-Pee Dee Belemnite; V-SMOW, Vienna-Standard Mean Ocean Water.

All the carbonate samples show similar C-O compositions. $\delta^{18}O_{V\text{-}SMOW}$ values vary from 19.7‰ to 23.4‰ and $\delta^{13}C_{V\text{-}PDB}$ values were between −3.6‰ and −7.7‰. All the samples plotted within the field of limestones and marbles (Hudson, 1977; Baker et al., 1989), away from the field of primary mantle-derived carbonatites (Fig. 8).

5 Discussion

5.1 Evidence for an igneous origin of the carbonatite in West Junggar

The carbonate-rich rocks reported in West Junggar were developed in the Darbut and Baijiantan areas along the fault within the ophiolitic mélanges or the surrounding Carboniferous rocks. Compared with sedimentary carbonate and mantle-derived carbonatite, these carbonatites were characterized by low REEs content and enriched in Ba and Sr (Figs. 6, 7), similar to some sedimentary carbonates. However, several lines of evidence have demonstrated that these carbonate-rich rocks in West Junggar are magmatic carbonatite.

Firstly, the most important argument for an igneous origin of the carbonatites in West Junggar comes from both field and microscopic observations. In Baijiantan, the effusive carbonatites appear as circular-subcircular cones and mainly overlie the Baijiantan ophiolitic mélanges and surrounding Carboniferous strata along the fault (Fig. 2a). Chilled margin and flow structures are present in the carbonatites (Figs. 3a–c), signifying their magmatic origin. In Darbut, the carbonatites occur as dykes on various scales, cutting the components of the Darbut ophiolitic mélanges and some Carboniferous rocks (Figs. 2b, 3d–f). The second line of evidence is the presence of enstatite, chromite and magnetite phenocrysts which also indicates the magmatic crystallization of these rocks (Fig. 4).

Furthermore, the petrographic characteristics of the zircons from the carbonatites provide another important piece of evidence supporting an igneous origin. Most of the zircon grains from the carbonatites are euhedral and show oscillatory zoning (Fig. 5a). Oscillatory zoning is a typical feature commonly associated with magmatic rocks, resulting from physical/chemical disequilibrium during crystal growth and a quasi-cyclic alternation in composition (Shore and Fowler, 1996). No metamorphic mineral or hydrothermal halo is observed in these carbonatites, ruling out the possibility of a metamorphic or hydrothermal origin. The zircons have a good linear relationship between Th and U, which is also consistent with an igneous origin. The SHRIMP U-Pb dating of the zircons obtained an Eocene age of 39.7 ± 1.3 Ma, which is much later than the surrounding Carboniferous rocks. No contemporaneous magmatism has been identified in West Junggar. The zircons thus were not derived from the wall-rocks or formed during the crystallization of the carbonatites. this date also implies that these carbonatites are not chemically associated with the ophiolitic mélanges and Carboniferous wall-rocks. Therefore, the carbonate-rich rocks in West Junggar are magmatic in origin, based on their occurrence in the field, as well as mineralogical and textural characteristics.

5.2 Petrogenesis of the carbonatite

Carbonatites across the globe are commonly associated with melilitite, nephelinite, aillikite and kimberlite clans (Mitchell, 2005), originating from diverse mantle-derived magmas (e.g. Santosh and Omori, 2008; Pirajno et al., 2015; Sharygin et al., 2015). However, it has also been noted that there are carbonatite localities that are not associated with the above silicate rocks (Woolley, 2003), which are similar to the carbonatites in West Junggar. Two alternative explanations for the absence of silicate rocks have previously been proposed. One attributes the absence to non-exposure of the deeper parts of a parental plutonic complex (e.g. Garson, 1956). The other suggestion is that there are actually no associated silicate rocks with a genetic relationship with carbonatites and the carbonatites represent primary partial melts (Gittins and Harmer, 2003).

Eocene carbonatites in West Junggar occur mainly along the major structural units of the Darbut and Baijiantan ophiolitic belts. Coeval mantle-derived

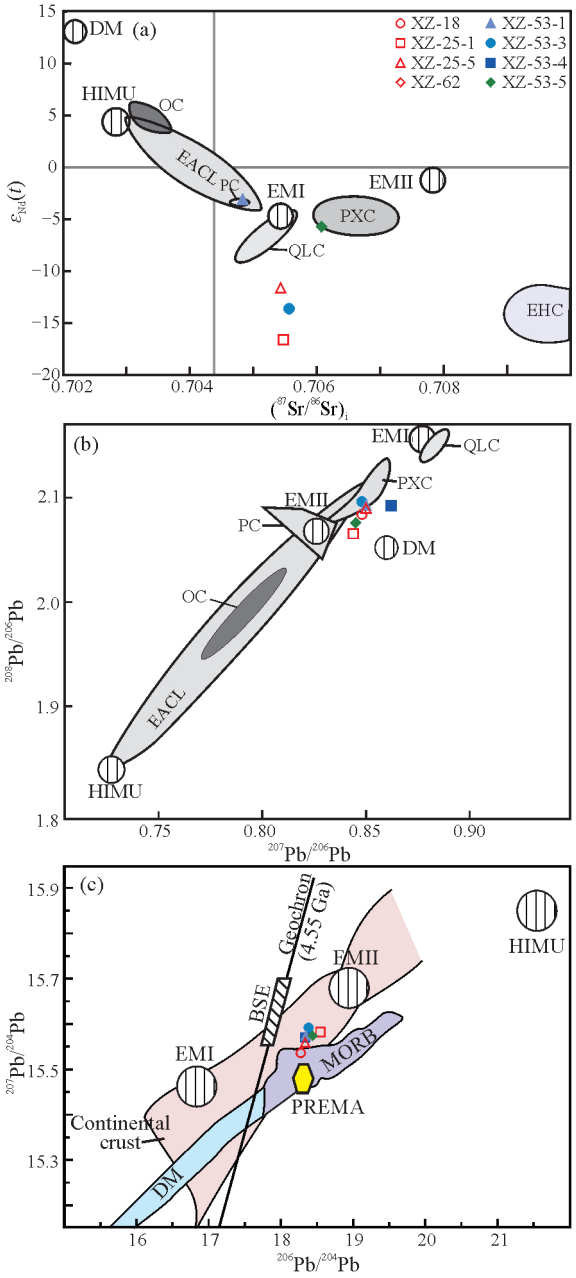

Fig. 7. (a) Initial value of $^{87}Sr/^{86}Sr$ versus $\varepsilon_{Nd}(t)$, (b) $^{207}Pb/^{206}Pb$ versus $^{208}Pb/^{206}Pb$, and (c) $^{207}Pb/^{204}Pb$ versus $^{206}Pb/^{204}Pb$ diagrams for the carbonatite from West Junggar.
All Pb isotopic ratios have been corrected for postcrystallization decay of U and Th. Range of mantle types from Zindler and Hart, 1986; EACL, East African Carbonatite Line (Bell and Tilton, 2001); EHC, carbonatite within eastern Himalayan syntaxis (Liu et al., 2006); OC, oceanic carbonatites from the Cape Verde and Canary Islands (Hoernle et al., 2002); PC, 30 Ma Pakistan carbonatites in a collision zone (Tilton et al., 1998); PXC, Panxi carbonatites in a collision zone (Hou et al., 2006); QLC, Late Triassic Qinling carbonatite dykes (Xu et al., 2011).

intrusive or extrusive silicate rocks with carbonatites have yet to be reported or observed in West Junggar, such as alkaline silicate rocks or kimberlite. Mineralogically, the carbonatites in West Junggar are mainly composed of carbonate minerals, quartz, enstatite, as well as accessory chromite, spinel, magnetite and apatite. They do not contain any typical alkaline minerals or REE-bearing minerals, making it unreasonable to argue for the existence of deeper parts of silicate rocks. The carbonatites in West Junggar possess the characteristics of primary magmatic melts.

The carbonatites in West Junggar are low in REEs with a flat pattern and lack anomalies of Zr and Hf, as distinct from the mantle-derived carbonatites worldwide (e.g. Bizimis, 2001; Pirajno, 2015) that are characterized by a high abundance of LREE, high LREE/HREE ratios and depletions of Zr, Hf and Ti (Fig. 6b). On the other hand, the carbonatites in West Junggar show Nb depletion, a widespread feature of continental rocks (Pearce, 1983). The alkaline contents are also relatively low, similar to some sedimentary carbonate rocks.

The carbonatites in West Junggar yield negative $\varepsilon_{Nd}(t)$ values of −2.98 to −16.58 and high $(^{87}Sr/^{86}Sr)_i$ values from 0.7048 to 0.7061, which differ from those of well-established mantle-derived carbonatites (Fig. 7a). The mantle-derived carbonatites (Fig. 7a) either fall on the HIMU-EMI mixing line in the $\varepsilon_{Nd}(t)$–$(^{87}Sr/^{86}Sr)_i$ diagram, e.g. East African Carbonatite Line (EACL) defined by Bell and Blenkinsop (1987, 1989), or in the HIMU-EMI-EMII field, indicating metasomatism with crustal material in the origin. Similar to the carbonatites in West Junggar, carbonatites within the eastern Himalayan syntaxis (EHC) reported by Liu et al. (2006) are also distinct from the mantle-derived carbonatite fields outlined in Figure 7a, which have been proposed to be generated from the partial melting of impure metasedimentary marbles. Similar to the Sr-Nd isotopic analyses, carbonatites in West Junggar also fall off the line defined by mantle-derived carbonatites (Fig. 7b), with a lower $^{208}Pb/^{206}Pb$ ratio, which is consistent with the lower Th concentration of mantle-derived carbonatites (Fig. 6b). Instead, the Pb isotopes of carbonatites in West Junggar fall in the continental field in the $^{207}Pb/^{204}Pb$-$^{206}Pb/^{206}Pb$ diagram (Fig. 7c). In addition, the carbonatites in West Junggar have typical $\delta^{18}O_{V\text{-}SMOW}$ and $\delta^{13}C_{V\text{-}PDB}$ values of limestones/marbles (Fig. 8). Therefore, it is beyond reasonable doubt that continental limestones/marbles contributed to the primary magmas of the carbonatites in West Junggar.

As noted above, the carbonatites in West Junggar are markedly distinct from mantle-derived carbonatites. The trace-element and isotopic characteristics of the carbonatites in West Junggar favor a crustal source similar to those reported in the eastern Himalayan syntaxis (Liu et al., 2006) and Daqinshan, North China Craton (Wan et al., 2008). Liu et al. (2006) reported that the carbonatites from the eastern Himalayan syntaxis were poor in REEs, Ba, Sr, U, Th, Nb and have different isotopic compositions from those of mantle-derived carbonatite. It was interpreted that the carbonatites were formed by fluxing limestones at a high temperature, which was triggered by the extrusion of the Greater Himalayan Crystallines into the overlying limestone/marble-bearing Lesser Himalayan Crystallines. Similar findings were also reported in the Daqinshan area, Western Block of the North China Craton, where they were interpreted to be formed by the anatexis of impure marble from amphibolite-granulite facies Archean

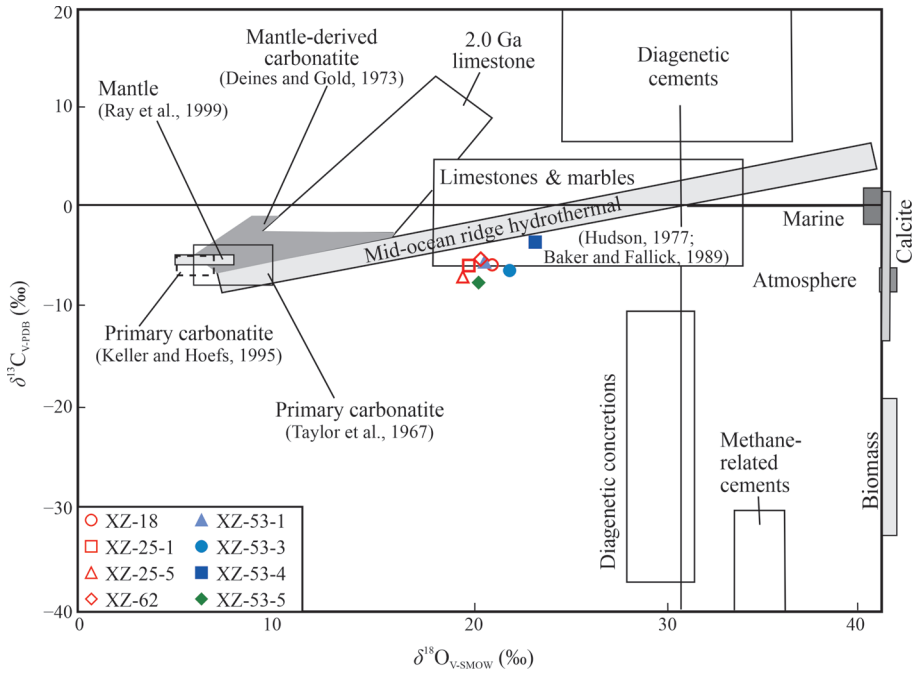

Fig. 8. C-O isotopes of the carbonatites from West Junggar (boundaries modified after Rollinson, 1993).

khondalite series under a high geothermal gradient (Wan et al., 2008).

Experimental data show that partial melting of limestone would occur when the temperature reaches 740°C at 1 kbar in the presence of water. The melting process could also be enhanced with the addition of small amounts of CO_2, according to high-P-T experiments in the CaO-CO_2-H_2O (Wyllie and Tuttle, 1960) and MgO-CaO-CO_2-H_2O systems (Fanelli et al., 1986). Moreover, the addition of MgO to the CaO-H_2O-CO_2 system will result in the decrease of the eutectic temperature to as low as around 600°C (Fanelli et al., 1986). Therefore, the idea that carbonatite magma originated at crustal levels from the melting of sedimentary carbonates is supported by these experimental results. Moreover, there is no crystalline basement in West Junggar, only a Carboniferous remnant basin with overlying basalt, peperite and carbonate sediments (Chen et al., 2014), which provide the source rock of the West Junggar carbonatites. SHRIMP U-Pb ages of inherited cores in zircons are Carboniferous in age (Table 1), also confirming that the Carboniferous carbonates should be the source rock of the carbonatites.

In summary, it is interpreted that the carbonatites in West Junggar were produced by the anatexis of Carboniferous sedimentary carbonates at crustal levels, so can reasonably be referred to as crustal carbonatites. The variations in the mineral or chemical composition of the crustal carbonatite might be related to the original impure source being influenced by calc-silicates and other crustal material.

5.3 Tectonic implications

Intracontinental anorogenic carbonatites commonly occur in rift-related environments, best exemplified by the East African Rift (e.g., Bell and Tilton, 2001; Pirajno, 2015) and some (post-) collisional settings (e.g. Chakhmouradian et al., 2008; Xu et al., 2011). These mantle-derived carbonatites usually show close spatial and temporal relationships with other mantle-derived silicate rocks (Pirajno, 2015). In contrast to that scenario, no contemporaneous mantle-derived silicate rocks have yet been found in West Junggar and North Xinjiang. As discussed above, Eocene crustal carbonatites in West Junggar originated from the melting of Carboniferous sedimentary carbonates at crustal levels.

The Baijiantan and Darbut ophiolitic mélanges are interpreted to originate from two parallel crustal-scale strike-slip fault zones within a remnant ocean basin, not major plate boundaries nor subduction-suture zones (Chen et al., 2014). The remnant ocean basin was trapped and preserved in West Junggar, following regional collisions and the bending of the Kazakhstan orocline during the Late Devonian to Early Carboniferous (Chen et al., 2014). Throughout the Carboniferous, the palaeo-remnant ocean basin was infilled with shallowing-upward sedimentary successions including the Tailegula, Baogutu and Xibeikulasi formations (from bottom to top). The crustal-scale strike-slip fault zones were triggered by a relative motion between the Junggar Block and the West Junggar remnant ocean basin in regional collisions during the Late Devonian to Carboniferous. These two fault zones tectonically disrupted the mafic oceanic crust and basin-fill sediments, as well as the ultramafic protrusions along the fault zones (Chen et al., 2014). Oceanic sedimentary carbonates are plentiful in the basin-fill successions, especially in the bottom carbonate sediments interacting with basalt as the matrix of peperite-bearing successions in the paleo-ocean floor.

The crustal carbonatite in West Junggar is a significant discovery for Cenozoic magmatism in Xinjiang. North

Xinjiang evolved into an intraplate setting after the Permian and its magmatic activity tended to be subdued after the Paleozoic. Recently, several Cenozoic magmatic events have been reported in North Xinjiang, such as basalt outcrops in Halaqiaola, Artai and mafic assemblages in Tuoyun, Southwestern Tianshan (Zhang et al., 2007; Simonov et al., 2008). The Halaqiaola basalt along the Keketuohai-Ertai Fault yields a K-Ar date of 10–18 Ma, originating from an enriched mantle source (Huang et al., 2006; Zhang et al., 2007). The Tuoyun mafic assemblages outcrop to the east of the Talas-Fergana Fault and are composed of olivine basalt, gabbro, diabase, pyroxene peridotite and phonolite. The basalt occurs as lava flows and the intrusive rocks occur as dykes and sheets along the sedimentary strata (Ji et al., 2006). All these mafic rocks were interpreted to be derived from enriched lithospheric mantle with some crustal contamination (Ji et al., 2006, Simonov et al., 2008). The lower unit of the Tuoyun mafic assemblages was dated between 102–122 Ma and the upper unit was developed in the time range from 76 Ma to 40 Ma (Han et al., 1998; Sobel and Arnaud, 2000; Wang et al., 2000; Huang et al., 2005; Ji et al., 2006; Liang et al., 2007; Simonov et al., 2008).

In general, Cenozoic magmatism was not widely developed in North Xinjiang, except for a few sporadic exposures, each less than 10 km^2 in the outcrop area (Fig. 9). However, all these small-scale Cenozoic magmatic localities are universally distributed along the regional Cenozoic strike-slip faults or fault intersections (Fig. 9). For example, the Talas-Fergana Fault, where the Tuoyun mafic assemblages are located, is a Mesozoic–Cenozoic NW-tending dextral strike-slip fault. In Altai, the Irtysh Fault and the Keketuohai-Ertai Fault as two major strike-slip faults were activated due to the intracontinental dextral shear state of stress (Laurent-Charvet, 2002). The Halaqiaola basalt erupted in the intersections of these two major strike-slip faults (Zhang et al., 2007; Huang et al., 2006). The occurrences of Cenozoic crustal carbonatites reported in this study are also constrained by crustal-scale fault zones represented by the Darbut and Baijiantan ophiolitic belt in West Junggar (Chen et al., 2014). From the timing of all of these Cenozoic magmatic events in North Xinjiang, they may have followed/accompanied the collision of the Indian and Eurasian continents, which has been variously reported as having started at 65 Ma (Yin and Harrison, 2000), ~60 Ma (Decelles et al., 2014) or ~50 Ma (Rowley et al., 1998; Najman et al., 2001, 2010; Zhu et al., 2005).

Therefore, we propose that the Cenozoic intraplate magmatism in North Xinjiang is due to the remote effect of the Indian-Eurasian collision. The collision triggered the activation of the major faults, mainly strike-slip faults, along with localized intraplate magmatism (Pirajno, 2010). First of all, these faults could provide pathways for the magmatism. Secondly, the activation of these faults enabled the decompressional melting of the underlying crust and continental lithospheric mantle (Pirajno, 2010). In this scenario, magma chambers and overlying volcanoes were likely positioned at extensional offsets in strike-slip faults or at the intersection of other fault lineaments (e.g., McNulty et al., 1998; Acocella and Funiciello, 2010; Shabanian et al., 2012). The fact that the occurrences of Cenozoic magmatism in North Xinjiang are mainly along the strike-slip faults or fault intersections confirms this mechanism, in a manner analogous to that described for a type of post-collisional setting in Iran by Shabanian et al. (2012).

In West Junggar, the reactivation of the Darbut and Baijiantan crustal-scale strike-slip fault zones caused by the Indian-Eurasian collision enables the decompression melting of underlying lithospheric mantle. The resulting magmatic melt was then injected through the strike-slip faults and transferred a considerable amount of thermal energy to the lower crust. The heat would have caused partial melting of the carbonate sediments at the bottom of the Carboniferous remnant ocean basin-fill successions and consequently formed the source magma of the crustal carbonatites in West Junggar (Fig. 10). Therefore, the crustal carbonatites in West Junggar provide new evidence for Cenozoic magmatism in North Xinjiang and are also significant for the investigation of tectono-magmatic relations and crust-mantle interaction in North Xinjiang and the CAOB.

6 Conclusions

The crustal carbonatites in West Junggar are mainly distributed in the Darbut and Baijiantan ophiolitic mélanges. The effusive carbonatites in Baijiantan occur as a series of circular to subcircular cones overlying the mélanges and Carboniferous successions. The intrusive carbonatites occur either as steeply-dipping dykes along the margins of the Darbut ophiolitic mélange or cross-cut the components of the mélanges. Chilled margin and flow structures are present in the carbonatites.

SHRIMP zircon U-Pb dating shows the crustal carbonatites in West Junggar were formed at an Eocene age of 39.7 ± 1.3 Ma.

The crustal carbonatites in West Junggar are igneous in origin and differ from mantle-derived carbonatites. They are poor in REEs, Th, U, Nb and Ta. They have extremely low $\varepsilon_{Nd}(t)$, high $(^{87}Sr/^{86}Sr)_i$ ratios, high $\delta^{18}O_{V\text{-}SMOW}$ values and relatively high $\delta^{13}C_{V\text{-}PDB}$ values, similar to those found in most sedimentary carbonates. Therefore, we propose that the crustal carbonatites in West Junggar originated from the melting of Carboniferous sedimentary carbonates at crustal levels.

The reactivation of the Darbut and Baijiantan crustal-scale strike-slip fault zones, initiated by the Indian-Eurasian collision, enabled the decompression melting of underlying continental lithospheric mantle. The resulting magmatic melts were injected through the strike-slip faults and transferred a considerable amount of heat energy to the lower crust, which caused the partial melting of the Carboniferous carbonate sediments and consequently formed the source magma of the crustal carbonatites in West Junggar.

Acknowledgements

This study is financially supported by the National Key Research and Development Plan (Grant No.

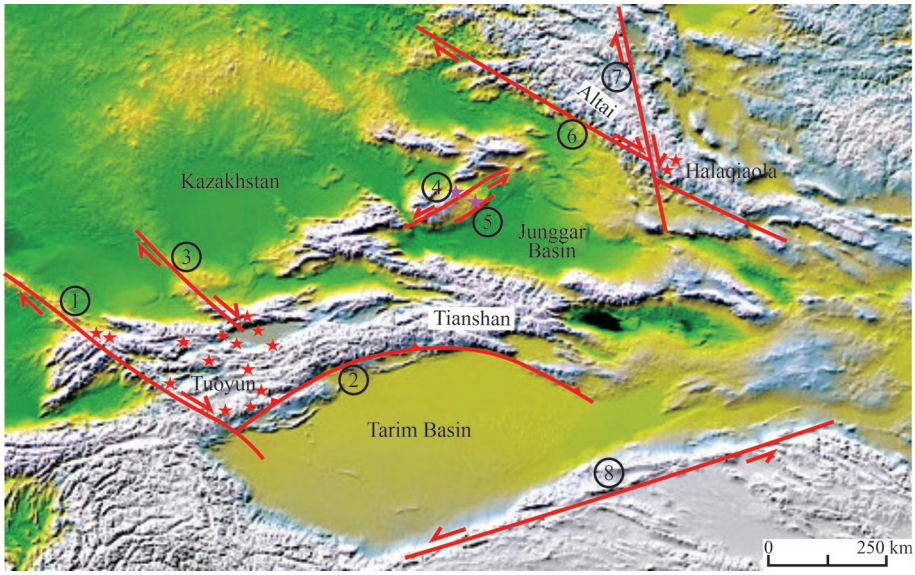

Fig. 9. Localities of Cenozoic intraplate basalts (stars) and regional large-scale strike-slip fault zones in the North Xinjiang region.
① Talas-Fergana Fault; ② North Tarim Fault; ③ Dzhalair-Naiman Fault; ④ Darbut Fault and Darbut ophiolitic mélange; ⑤ Baijiantan ophiolitic mélange; ⑥ Irtysh-Zaisan Fault. ⑦ Keketuohai-Ertai Fault; ⑧ Altyn Tagh Fault.

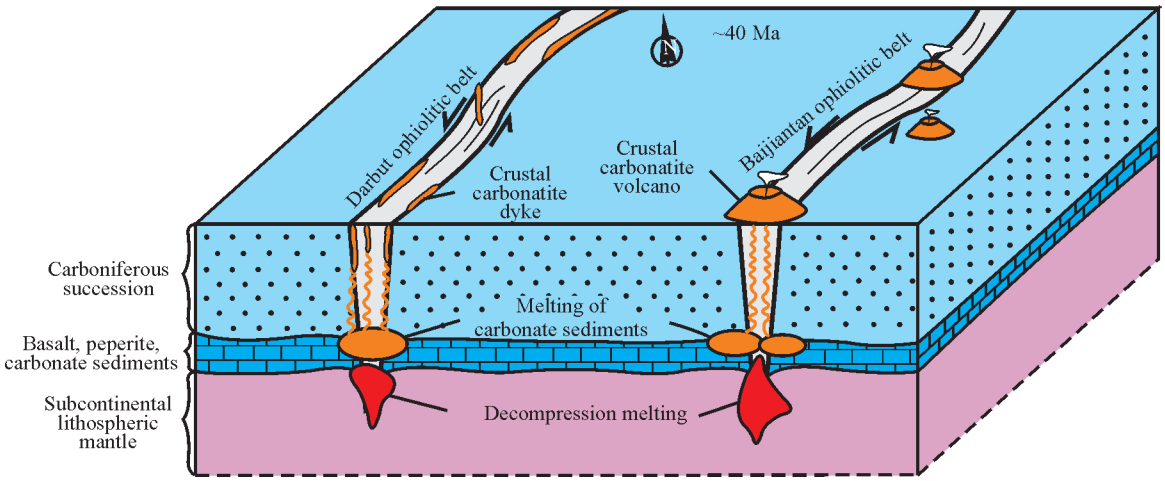

Fig. 10. Schematic diagram showing petrogenesis of the crustal carbonatites from West Junggar (not to scale).

2017YFC0603105). We gratefully acknowledge Dr. David J.W. Piper and Dr. Georgia Pe-Piper for their helpful discussion and kind assistance.

Manuscript received Feb. 03, 2019
accepted Apr. 23, 2020
associate EIC: FEI Hongcai
edited by Jeff LISTON and GUO Xianqing

Supplementary material to this article can be found online at http: //doi.org/10.1111/1755-6724.14772.

References

Acocella, V., and Funiciello, F., 2010. Kinematic setting and structural control of arc volcanism. Earth and Planetary Science Letters, 289: 43–53.

Allen, M.B., Şengör, A.M.C., and Natal'in, B.A., 1995. Junggar, Turfan and Alakol basins as Late Permian to Early Triassic extensional structures in a sinistral shear zone in the Altaid orogenic collage, Central Asia. Journal of the Geological Society, 152: 327–338.

Baker, A.J., and Fallick, A.E., 1989. Evidence from Lewisian limestones for isotopically heavy carbon in two-thousand-million-year-old sea water. Nature, 337: 352–354.

Bell, K., and Blenkinsop, J., 1987. Nd and Sr isotopic compositions of East African carbonatites: Implications for mantle heterogeneity. Geology, 15: 99–102.

Bell, K., and Blenkinsop, J., 1989. Neodymium and strontium isotope geochemistry of carbonatites. In: Bell, K. (ed.), Carbonatites: Genesis and Evolution. Unwin Hyman, London, 278–300.

Bell, K., Kjarsgaard, B.A., and Simonetti, A., 1998. Carbonatites—Into the Twenty-first Century. Journal of Petrology, 39: 1839–1845.

Bell, K., and Rukhlov, A.S., 2004. Carbonatites from the Kola alkaline province: Origin, evolution and source characteristics. In: Wall, F., Zaitsev, A.N. (eds.), Phoscorites and Carbonatites from Mantle to Mine: The Key Example of the Kola Alkaline Province. Mineralogical Society Series, London, 421–455.

Bell, K., and Tilton, G.R., 2001. Nd, Pb and Sr isotopic compositions of East African carbonatites: Evidence for mantle mixing and plume inhomogeneity. Journal of Petrology, 42: 1927–1945.

Bell, K., and Tilton, G.R., 2002. Probing the mantle: The story from carbonatites. Eos, Transactions American Geophysical Union, 83: 273–277.

Bizimis, M.S., 2001. Geochemical processes in the upper mantles: Evidence from peridotites, kimberlites and carbonatites (Ph. D thesis). Florida State University.

Chakhmouradian, A.R., Mumin, A.H., Demény, A., and Elliott, B., 2008. Postorogenic carbonatites at Eden Lake, Trans-Hudson Orogen (northern Manitoba, Canada): Geological setting, mineralogy and geochemistry. Lithos, 103: 503–526.

Chen, B., and Arakawa, Y., 2005. Elemental and Nd-Sr isotopic geochemistry of granitoids from the West Junggar foldbelt (NW China), with implications for Phanerozoic continental growth. Geochimica et Cosmochimica Acta, 69: 1307–1320.

Chen, H., Qu, X.M., Xin, H.B., and Jiang, J.H., 2010. A tentative discussion on the genesis of Ni-bearing carbonatites in the Bangong Lake area, Tibet. Mineral Deposit, 29: 1029–1042 (in Chinese with English abstract).

Chen, S., Guo Z.J., Pe-Piper, G., and Zhu, B.B., 2013. Late Paleozoic peperites in West Junggar, China, and how they constrain regional tectonic and palaeoenvironmental setting. Gondwana Research, 23: 666–681.

Chen, S., Pe-Piper, G., Piper, D.J.W., and Guo, Z.J., 2014. Ophiolitic mélanges in crustal-scale fault zones: Implications for the Late Palaeozoic tectonic evolution in West Junggar, China. Tectonics, 33: 2419–2443.

Choulet, F., Faure, M., Cluzel, D., Chen, Y., Lin, W., and Wang, B., 2012. From oblique accretion to transpression in the evolution of the Altaid collage: New insights from West Junggar, northwestern China. Gondwana Research, 21: 530–547.

Coleman, R.G., 1989. Continental growth of northwest China. Tectonics, 8: 621–635.

Compston, W., Williams, I.S., Kirschcink, J.L., Zhang Z.C., and Ma, G.G., 1992. Zircon U-Pb ages for the Early Cambrian time-scale. Journal of the Geological Society, 149: 171–184.

Dalton, J.A., and Wood, B.J., 1993. The compositions of primary carbonate melts and their evolution through wallrock reaction in the mantle. Earth and Planetary Science Letters, 119: 511–525.

DeCelles, P.G., Kapp, P., Gehrels, G.E., and Ding, L., 2014. Paleocene–Eocene foreland basin evolution in the Himalaya of southern Tibet and Nepal: Implications for the age of initial India-Asia collision. Tectonics, 33: 824–849.

Deines, P., 1989. Stable isotope variations in carbonatites. In: Bell, K. (ed.), Carbonatites: Genesis and Evolution. Unwin Hyman, London, 301–359.

Dong, C.Y., Liu, D.Y., Wan, Y.S., Xu, Z.Y., Liu, Z.H., and Yang, Z.S., 2009. Crustally-derived carbonatite from the Daqinshan area: Zircon features and SHRIMP dating. Acta Geologica Sinica, 83: 388–398 (in Chinese with English abstract).

Downes, H., Balaganskaya, E., Beard, A., Liferovich, R., and Demaiffe, D., 2005. Petrogenetic processes in the ultramafic, alkaline and carbonatitic magmatism in the Kola Alkaline Province: A review. Lithos, 85: 48–75.

Fanelli, M.T., Cava, N., and Wyllie, P.J., 1986. Calcite and dolomite without portlandite at a new eutectic in CaO-MgO-CO_2-H_2O with applications to carbonatites. In: Morphology and Phase Equilibria of Minerals, Proceedings of the 13th General Meeting of the International Mineralogical Association. Bulgarian Academy of Science, Sofia, 313–322.

Garson, M.S., 1956. Carbonatites in southern Malawi. Ministry of Natural Resources Geological Survey Department, Malawi.

Gittins, J., and Harmerm, R.E., 2003. Myth and reality in the carbonatite-silicate rock "association". Periodico Di Mineralogia, 72: 19–26.

Gu, P.Y., Li, Y.J., Zhang, B., Tong, L.L., and Wang, J.N., 2009. LA-ICP-MS zircon U-Pb dating of gabbro in the Darbut ophiolite, West Junggar, China. Acta Petrologica Sinica, 25: 1364–1372 (in Chinese with English abstract).

Hammouda, T., 2003. High-pressure melting of carbonated eclogite and experimental constraints on carbon recycling and storage in the mantle. Earth and Planetary Science Letters, 214: 357–368.

Han, B.F., Wang, X.C., He, G.Q., Wu, T.R., Li, M.S., Liu, Y.L. and Wang, S.G., 1998. Discovery of mantle lower crust xenoliths from Early Cretaceous volcanic rocks of southwestern Tianshan, Xinjiang. Chinese Science Bulletin, 43: 2554–2557 (in Chinese).

Hoernle, K., Tilton, G., Le Bas, M.J., Duggen, S., and Garbe-Schönberg, D., 2002. Geochemistry of oceanic carbonatites compared with continental carbonatites: Mantle recycling of oceanic crustal carbonate. Contributions to Mineralogy and Petrology, 142: 520–542.

Hou, Z.Q., Tian, S.L., Yuan, Z.X., Xie, Y.L., Yin, S.P., Yi, L.S., Fei, H.C., and Yang, Z.M., 2006. The Himalayan collision zone carbonatites in western Sichuan, SW China: Petrogenesis, mantle source and tectonic implication. Earth and Planetary Science Letters, 244: 234–250.

Hou, Z.Q., Liu, Y., Tian, S.H., Yang, Z.M., and Xie, Y.L., 2015. Formation of carbonatite related giant rare-earth-element deposits by the recycling of marine sediments. Scientific Reports, 5: 10231.

Huang, B.C., Piper, J.D.A., He, H.Y., Zhang, C.X., and Zhu, R.X., 2006. Paleomagnetic and geochronological study of the Halaqiaola basalts, southern margin of the Altai Mountains, northern Xinjiang: Constraints on neotectonic convergent patterns north of Tibet. Journal of Geophysical Research: Solid Earth, 111: B01101.

Huang, B.C., Piper, J.D.A., Wang, Y.C., He, H.Y., and Zhu, R.X., 2005. Paleomagnetic and geochronological constraints on the post-collisional northward convergence of southwest Tian Shan, NW China. Tectonophysics, 409: 107–124.

Hudson, J.D., 1977. Stable isotopes and limestone lithification. Journal of the Geological Society, 133: 637–660.

Jahn, B.M., Capdevila, R., Liu, D.Y., Vernon, A., and Badarch, G., 2004. Sources of Phanerozoic granitoids in the transect Bayanhongor–Ulaan Baatar, Mongolia: Geochemical and Nd isotopic evidence, and implications for Phanerozoic crustal growth. Journal of Asian Earth Sciences. 23: 629–653.

Ji, J.Q., Han, B.F., Zhu, M.F., Chu, Z.Y., and Liu, Y.L., 2006. Cretaceous–Paleogene alkaline magmatism in the Tuyon basin, southwest Tianshan mountains: Geochronology, petrology and geochemistry. Acta Petrologica Sinica, 22: 1324–1340 (in Chinese with English abstract).

Laurent-Charvet, S., Charvet, J., Shu, L.S., Ma, R.S., and Lu, H.F., 2002. Palaeozoic late collisional strike-slip deformations in Tianshan and Altay, eastern Xinjiang, NW China. Terra Nova, 14: 249–256.

Le Maiter, R.W., 2002. Igneous Rocks: A Classification and Glossary of Terms. Cambridge University Press, Cambridge, U.K., 1–252.

Liang, T., Luo, Z.H., Ke, S., Wei, Y., Li, D.D., Huang, J.X., and Huang, F., 2007. SHRIMP zircon dating of the Tuyon volcanoes group, Xinjiang, and its geodynamic implications. Acta Petrologica Sinica, 23(6): 1381–1391 (in Chinese with English abstract).

Liu, Y., and Hou, Z.Q., 2017. A synthesis of mineralization styles with an integrated genetic model of carbonatite-syenite-hosted REE deposits in the Cenozoic Mianning-Dechang REE metallogenic belt, the eastern Tibetan Plateau, southwestern China. Journal of Asian Earth Sciences, 137: 35–79.

Liu, Y., Berner, Z., Massonne, H.J., and Zhong, D.L., 2006. Carbonatite-like dykes from the eastern Himalayan syntaxis: Geochemical, isotopic, and petrogenetic evidence for melting of metasedimentary carbonate rocks within the orogenic crust. Journal of Asian Earth Sciences, 26: 105–120.

Liu, Y., Chen, Z.Y., Yang, Z.S., Sun, X., Zhu Z.M., and Zhang Q.C., 2015. Mineralogical and geochemical studies of brecciated ores in the Dalucao REE deposit, Sichuan Province, southwestern China. Ore Geology Reviews, 70: 613–636.

McNulty, B.A., Farber, D.L., Wallace, G.S., Lopez, R., and Palacios, O., 1998. Role of plate kinematics and plate-slip-vector partitioning in continental magmatic arcs: Evidence

from the Cordillera Blanca, Peru. Geology, 26: 827–830.
Mitchell, R.H., 2005. Carbonatites and carbonatites and carbonatites. The Canadian Mineralogist, 43: 2049–2068.
Najman, Y., Appel, E., Boudagher-Fadel, M., Bown, P., Carter, A., Garzanti, E., Godin, L., Han, J.T., Liebke, U., Oliver, G., Parrish, R., and Vezzoli, G., 2010. Timing of India-Asia collision: Geological, biostratigraphic, and palaeomagnetic constraints. Journal of Geophysical Research: Solid Earth, 115: B12416.
Najman, Y., Pringle, M., Godin, L., and Oliver, G., 2001. Dating of the oldest continental sediments from the Himalayan foreland basin. Nature, 410: 194–197.
Pearce, J.A., 1983. Role of the sub-continental lithosphere in magma genesis at active continental margins. In: Hawkesworth, C.J., and Norry, M.J. (eds.), Continental Basalts and Mantle Xenoliths. Nantwich, Shiva Publishing Limited, United Kingdom, 230–249.
Pirajno, F., 2010. Intracontinental strike-slip faults, associated magmatism, mineral systems and mantle dynamics: Examples from NW China and Altay-Sayan (Siberia). Journal of Geodynamics, 50: 325–346.
Pirajno, F., 2015. Intracontinental anorogenic alkaline magmatism and carbonatites, associated mineral systems and the mantle plume connection. Gondwana Research, 27: 1181–1216.
Ren, J.D., Lu, S.W., Pei, Z.C., Yang, J.F., Fang, H.B., Li, C.Y., and Chao, H.L., 2007. Igneous carbonatite in the Muji area, Artux, Xinjiang, China: Evidence from geological and geochemical analyses. Geological Bulletin of China, 26(12): 1665–1670 (in Chinese with English abstract).
Rollinson, H.R., 1993. Using geochemical data: Evolution, presentation, interpretation. Pearson Education Limited, Harlow.
Rosatelli, G., Wall, F., and Stoppa, F., 2007. Calcio-carbonatite melts and metasomatism in the mantle beneath Mt. Vulture (Southern Italy). Lithos, 99: 229–248.
Rowley, D.B., 1998. Minimum age of initiation of collision between India and Asia North of Everest based on the subsidence history of the Zhepure Mountain section. The Journal of Geology, 106: 220–235.
Santosh, M., and Omori, S., 2008. CO_2 windows from mantle to atmosphere: Models on ultrahigh-temperature metamorphism and speculations on the link with melting of snowball Earth. Gondwana Research, 14: 82–96.
Sengör, A.C., and Natal'in, B.A., 1996. Turkic-type orogeny and its role in the making of the continental crust. Annual Review of Earth and Planetary Sciences, 24: 263–337.
Sengör, A., Natal'in, B.A., and Burtman, V.S., 1993. Evolution of the Altaid tectonic collage and Palaeozoic crustal growth in Eurasia. Nature, 364: 299–307.
Shabanian, E., Acocella, V., Gioncada, A., Ghasemi, H., and Bellier, O., 2012. Structural control on volcanism in intraplate post collisional settings: Late Cenozoic to Quaternary examples of Iran and Eastern Turkey. Tectonics, 31: TC3013.
Sharygin, I.S., Litasov, K.D., Shatskiy, A., Golovin, A.V., Ohtani, E., and Pokhilenko, N.P., 2015. Melting phase relations of the Udachnaya-East Group-I kimberlite at 3.0–6.5 GPa: Experimental evidence for alkali-carbonatite composition of primary kimberlite melts and implications for mantle plumes. Gondwana Research, 28: 1391–1414.
Shore, M., Fowler, A.D., 1996. Oscillatory zoning in minerals: A common phenomenon. The Canadian Mineralogist, 34: 1111–1126.
Simonov, V.A., Mikolaichuk, A.V., Rasskazov, S.V., and Kovyazin, S.V., 2008. Cretaceous–Paleogene within-plate magmatism in Central Asia: Data from the Tien Shan basalts. Russian Geology and Geophysics, 49: 520–533.
Sobel, E.R., and Arnaud, N., 2000. Cretaceous–Paleogene basaltic rocks of the Tuyon basin, NW China and the Kyrgyz Tian Shan: The trace of a small plume. Lithos, 50: 191–215.
Solovova, I.P., Girnis, A.V., Kogarko, L.N., Kononkova, N.N., Stoppa, F., and Rosatelli, G., 2005. Compositions of magmas and carbonate-silicate liquid immiscibility in the Vulture alkaline igneous complex, Italy. Lithos, 85: 113–128.
Steiger, R.H., and Jäger, E., 1977. Subcommission on geochronology: Convention on the use of decay constants in geo- and cosmochronology. Earth and Planetary Science Letters, 36: 359–362.
Sun, S.S., and McDonough, W.F., 1989. Chemical and isotopic systematics of oceanic basalts: Implications for mantle composition and processes. In: Saunders, A.D., Norry, M.J. (eds.), Magmatism in the Ocean Basins. Geological Society of London, Special Publication, 42: 313–345.
Tilton, G.R., Bryce, J.G., and Mateen, A., 1998. Pb-Sr-Nd isotope data from 30 and 300 Ma collision zone carbonatites in northwest Pakistan. Journal of Petrology, 39: 1865–1874.
Tuttle, O.F., and Gittins, J., 1966. Carbonatites. New York: Wiley, 1–592.
Veksler, I.V., Petibon, C., Jenner, G.A., Dorfman, A.M., and Dingwell, D.B., 1998. Trace element partitioning in immiscible silicate-carbonate liquid systems: An initial experimental study using a centrifuge autoclave. Journal of Petrology, 39: 2095–2104.
Wan, Y.S., Liu, D.Y., Xu, Z.Y., Dong, C.Y., Wang, Z.J., Zhou, H.Y., Yang, Z.S., Liu, Z.H., and Wu, J.S., 2008. Paleoproterozoic crustally derived carbonate-rich magmatic rocks from the Daqinshan area, North China Craton: Geological, petrographical, geochronological and geochemical (Hf, Nd, O and C) evidence. American Journal of Science, 308: 351–378.
Wang, Y.B., Wang, Y., Liu, X., Fu, D.R., Xiao, X.C., and Qi, L.S., 2000. Geochemical characteristics and genesis of Late Cretaceous to Paleoene basalts in Tuyon Basin, South Tianshan Mountain. Acta Petrologica et Mineralogica, 19(2): 131–139 (in Chinese with English abstract).
Windley, B.F., Alexeiev, D., Xiao, W.J., Kröner, A., and Badarch, G., 2007. Tectonic models for accretion of the Central Asian Orogenic Belt. Journal of the Geological Society, 164: 31–47.
Woolley, A.R., 2003. Igneous silicate rocks associated with carbonatites: Their diversity, relative abundances and implications for carbonatite genesis. Periodico Di Mineralogia, 72: 9–17.
Wyllie, P.J., and Tuttle, O.F., 1960. The system CaO-CO_2-H_2O and the origin of carbonatites. Journal of Petrology, 1: 1–46.
XBGMR, 1966. Introduction of geological map of Karamay area. Map scale at 1: 200000. Xinjiang Bureau of Geology and Mineral Resources, Xinjiang.
Xiao, W.J., Han, C.M., Yuan, C., Sun, M., Lin, S.F., Chen, H.L., Li, Z., Li, J.L., and Sun, S., 2008. Middle Cambrian to Permian subduction-related accretionary orogenesis of Northern Xinjiang, NW China: Implications for the tectonic evolution of central Asia. Journal of Asian Earth Sciences, 32: 102–117.
Xiao, W.J., Han, C.M., Yuan, C., Sun, M., Lin, S.F., Chen, H.L., Li, Z., Li, J.L., and Sun, S., 2010. A review of the western part of the Altaids: A key to understanding the architecture of accretionary orogens. Gondwana Research, 18: 253–273.
Xie, X.J., Yan, M.C., Li, L.Z., and Shen, H.J., 1985. Usable values for Chinese standard reference samples of stream sediments, soils, and socks: GSD 9-12, GSS 1-8 and GSR 1-6. Geostandards and Geoanalytical Research, 9: 277–280.
Xu, C., Chakhmouradian, A.R., Taylor, R.N., Kynicky, J., Li, W.B., Song, W.L., and Fletcher, I.R., 2014. Origin of carbonatites in the South Qinling orogen: Implications for crustal recycling and timing of collision between the South and North China Blocks. Geochimica et Cosmochimica Acta, 143: 189–206.
Xu, C., Taylor, R.N., Kynicky, J., Chakhmouradian, A.R., Song, W.L., and Wang, L.J., 2011. The origin of enriched mantle beneath the North China block: Evidence from young carbonatites. Lithos, 127: 1–9.
Xu, X., He, G.Q., Li, H.Q., Ding, T.F., Liu, X.Y., and Mei, S.W., 2006. Basic characteristics of the Karamay ophiolitic mélange, Xinjiang, and its zircon SHRIMP dating. Geology in China, 33: 470–475 (in Chinese).
Yakubchuk, A., 2004. Architecture and mineral deposit settings of the Altaid orogenic collage: A revised model. Journal of Asian Earth Sciences, 23: 761–779.
Yi, Z.Y., Huang, B.C., Xiao, W.J., Yang, L.K., and Qiao, Q.Q.,

2015. Paleomagnetic study of Late Paleozoic rocks in the Tacheng Basin of West Junggar (NW China): Implications for the tectonic evolution of the western Altaids. Gondwana Research, 27: 862–877.

Yin, A., and Harrison, T.M., 2000. Geologic Evolution of the Himalayan-Tibetan Orogen. Annual Review of Earth and Planetary Sciences, 28: 211–280.

Zhang, C., and Huang, X., 1992. Age and tectonic settings of ophiolites in West Junggar, Xinjiang. Geological Review, 38: 509–524 (in Chinese with English abstract).

Zhang, J.E., Xiao, W.J., Han, C.M., Ao, S.J., Yuan, C., Sun, M., Geng, H.Y., Zhao, G.C., Guo, Q.Q., and Ma, C., 2011. Kinematics and age constraints of deformation in a Late Carboniferous accretionary complex in Western Junggar, NW China. Gondwana Research, 19: 958–974.

Zhang, Y.Y., Guo, Z.J., Liu, C., and Xu, W.Q., 2007. Geochemical characteristics and geological implications of Cenozoic basalts, East Altai, Xinjiang. Acta Petrologica Sinica, 23(7): 1730–1738 (in Chinese with English abstract).

Zhao, B., Zhao, J.S., Wang, J.C., Ni, P., Li, Z.L., Rao, B., Lu, T.S., Shao, J.Z., Zhang, C.Z., Wang, R., Peng, Z.L., Tu, X.L., and Chen, L.L., 2004. A possible new carbonatite type: Crust-derived carbonatite. Geochimica, 33: 650–662 (in Chinese with English abstract).

Zhu, B., Kidd, W.S. F., Rowley, D.B., Currie, B.S., and Shafique, N., 2005. Age of Initiation of the India-Asia collision in the East–Central Himalaya. The Journal of Geology, 113: 265–285.

Zindler, A., and Hart. S.R., 1986. Chemical geodynamics. Annual Review of Earth and Planetary Sciences, 14: 493–571.

About the first and corresponding author

CHEN Shi, male; born in 1986 in Gansu Province; graduated from Peking University in 2008, received Ph.D. from Peking University in 2013, Associate Professor of the Chinese University of Petroleum (Beijing). He is currently interested in regional tectonics, volcanology, petrology and rock geochemistry. Email: chenshi4714@163.com.